



## Dynamics and internal structure of a lower mantle plume conduit

Cinzia G. Farnetani<sup>a,\*</sup>, Albrecht W. Hofmann<sup>b,c</sup>

<sup>a</sup> *Equipe de dynamique des fluides géologiques, Institut de Physique du Globe de Paris, and Université Paris Diderot, 4, pl. Jussieu, 75252 Paris, France*

<sup>b</sup> *Max-Planck-Institut für Chemie, Postfach 3060, 55020 Mainz, Germany*

<sup>c</sup> *Lamont-Doherty Earth Observatory, Columbia University New York, NY, USA*

### ARTICLE INFO

#### Article history:

Received 5 December 2008

Received in revised form 11 March 2009

Accepted 19 March 2009

Available online 21 April 2009

Editor: R.W. Carlson

#### Keywords:

mantle plumes

D<sup>7</sup>

geochemical heterogeneity

Hawaiian plume

### ABSTRACT

Geochemical studies, including those made possible by the Hawaiian Scientific Drilling Project, have revealed the chemically and isotopically heterogeneous nature of hotspot lavas, yet their interpretation is highly controversial and there is little agreement as to how geochemical heterogeneities might be spatially arranged within the plume conduit. To address this issue we conduct high resolution numerical simulations of an axisymmetric purely thermal plume, focusing on the lower mantle part of the conduit and on the thermal boundary layer (TBL) feeding the plume. We explore the relation between length-scales of heterogeneities across the source region and the length- and time-scales of geochemical variations in the plume conduit. The vertical velocity inside the conduit decreases exponentially with the square of radial distance generating high strain rates (order  $10^{-13}$ – $10^{-14}$  s<sup>-1</sup>) that modify the shape of upwelling heterogeneities into elongated and narrow filaments. Therefore, the preservation of 'blob-like' heterogeneities (i.e., with a 1:1 aspect ratio in a vertical section) is quite unlikely, even in the central part of the plume. For example, initial lenses of size  $100 \times 10$  km in the TBL are stretched into filaments 500–1000 km long. These filaments constitute 'long-lived' structures in a rising plume, and their geochemical fingerprints may be registered at a given radial distance for several millions of years. We also consider an idealized heterogeneous architecture inside the TBL, consisting of 'trains' of small scale lenses. When such trains upwell in the conduit, they form high radial geochemical gradients. Their 'geochemical record', registered over time at a given depth and radial distance, will fluctuate over time, with shorter period and a larger amplitude at the conduit center than at its periphery. Finally, we demonstrate that material existing 'side by side' in the conduit originated from regions in the TBL that are separated by distances of several hundred kilometers. This implies that vigorous plumes are able to sample, and to bring side by side, very distant portions of their source region. Our results provide a fluid dynamically consistent framework to discuss the main aspects of the different (and to some extent mutually exclusive) models of conduit structure used to interpret the geochemical observations of the Hawaiian lavas.

© 2009 Elsevier B.V. All rights reserved.

### 1. Introduction

Geochemical studies of Hawaiian basalts have yielded a wealth of data relevant to the understanding of the chemical and isotopic internal structure of mantle plumes. However, the interpretation of these data has remained highly controversial, partly because there are significant uncertainties as to how the volcanic plumbing system samples the underlying plume, but also because there is little agreement as to how the existing geochemical heterogeneities might be spatially arranged within the plume conduit. The pioneering model by Hauri et al. (1994), suggested a concentrically zoned plume conduit, whereby geochemical variations occur only in the radial direction, due to entrainment of surrounding mantle. Entrainment is governed by thermal diffusion and is expected to decrease with increasing plume flux

(Hauri et al., 1994). In spite of the high buoyancy flux of the Hawaiian plume (Sleep, 1990) the concentric model has been extensively invoked to explain the time and space variability of isotope ratios e.g., (DePaolo and Stolper, 1996; Hauri et al., 1996; Lassiter et al., 1996). However, recent data from the Hawaiian Scientific Drilling Project HSDR-2, have shown spatial and temporal variations for Pb, Nd, Hf, and Sr isotope ratios (see DePaolo et al., 2001; Blichert-Toft et al., 2003; Eisele et al., 2003; Abouchami et al., 2005; Bryce et al., 2005) and references therein) that are inconsistent with concentric zoning and have prompted the suggestion of new conceptual models.

Presenting a contrasting view of the internal plume structure, Blichert-Toft et al. (2003) propose a plume structure that minimizes radial variations across the conduit by assuming a 'plug-flow', whereby the vertical velocity remains nearly constant across the main part of the conduit and decreases sharply only at its periphery. The 'plug-flow' velocity profile contrasts with the exponentially varying velocity profile derived analytically by Olson et al. (1993). According to Blichert-Toft et al. (2003) the geochemical cross section of the plume does not

\* Corresponding author.

E-mail addresses: [cinzia@ipgp.jussieu.fr](mailto:cinzia@ipgp.jussieu.fr) (C.G. Farnetani), [hofmann@mpch-mainz.mpg.de](mailto:hofmann@mpch-mainz.mpg.de) (A.W. Hofmann).

need to be time invariant, so that the conduit structure may be similar to a stack of nearly horizontal thin ‘layers’ with distinct isotope ratios.

In yet another interpretation (Eisele et al., 2003; Abouchami et al., 2005) the conduit internal structure is similar to a bundle of vertically elongated filaments, successively sampled by different volcanoes as the Pacific plate moves over the Hawaiian plume. The underlying physical process is stretching of deep heterogeneities due to velocity gradients within the plume conduit.

The above interpretations are purely based on geochemical observations and there is a clear need to investigate the internal structure of a plume conduit from a fluid dynamics perspective. In this paper we use numerical simulations of a thermal plume to address some fluid dynamics questions expected to be relevant for the geochemical interpretation of internal plume structure. First, what is the relation between length-scales of heterogeneities across the source region (assumed to be the  $D''$  layer overlying the core–mantle boundary) and length- and time-scales of geochemical variations once heterogeneities are upwelling in the plume conduit? Second, deep heterogeneities may be thought of as isolated finite-size volumes, or they may be distributed in space so as to form an internal architecture in the  $D''$  region. In this case, what would be the internal structure of a plume conduit fed by such a complex source region? Third, are there fundamental differences between the central and the peripheral zones of the plume conduit, for example due to different deformations undergone during upwelling and/or different parts of the source region being sampled? Finally, which aspects of the three different (and to some extent mutually exclusive) models of conduit structure presented above are consistent with fluid dynamics constraints?

To our knowledge, previous fluid dynamics studies have not explored the relation between finite-size heterogeneities in the thermal boundary layer (TBL) and the conduit internal structure. Although it is beyond the scope of our paper to review the important contributions of laboratory experiments and numerical models for the understanding of mantle plumes, we note that early laboratory experiments, for example by Griffiths and Campbell (1990), focused on the plume head rather than on the long lived conduit. Moreover, laboratory experiments have rigid bottom boundary conditions and the hot plume is often injected in the tank, thereby precluding any investigation of the dynamics and internal deformations in the basal TBL. More recent experiments by Kerr and Mériaux (2004) on plumes upwelling in a mantle wind generated by surface plate motion, concluded that the Hawaiian plume conduit should be zoned azimuthally, rather than concentrically. However, Kerr and Mériaux (2004) did not consider the deformations of finite-size heterogeneities, nor did they quantify strain rates across the conduit and the TBL.

Our work is based on a purely thermal flow within an idealized TBL and the associated plume conduit. Certainly, the  $D''$  region is more complex than a thermal boundary layer (see for example Jellinek and Manga, 2004; Garnero and McNamara, 2008, and references therein), and our model does not include most of the recent findings, namely the post-perovskite phase transition (Murakami et al., 2004) and the existence of chemical heterogeneities in the deep mantle. While the role of the post-perovskite on mantle plumes is still a matter of debate, it is now clear that chemically denser material plays an important role on plumes shape and dynamics (Tackley, 1998; Davaille, 1999; Farnetani and Samuel, 2005), composition (Christensen and Hofmann, 1994; Samuel and Farnetani, 2003) and excess temperature (Farnetani, 1997). We are aware that considering the  $D''$  region as a purely thermal boundary layer is a gross simplification; nevertheless, from a modeling stand point, we consider it important and instructive to start with the most basic fluid flow.

It is also difficult to characterize the geochemical fingerprint of the  $D''$  region. The base of the Earth's mantle is likely to be a slab ‘graveyard’. In such a case, denser subducted crust may segregate and evolve geochemically (Christensen and Hofmann, 1994) before being recycled in mantle plumes (Hofmann and White, 1982). But the  $D''$

region, or parts of it, could also host a ‘hidden reservoir’, with a distinct geochemical composition, remnant from the early differentiation of the Earth's mantle (Boyet and Carlson, 2005; Tolstikhin and Hofmann, 2005). Deliberately, we do not attempt to reproduce this complex geochemistry and geochemical evolution over time. Instead, we conduct a ‘thought experiment’ to investigate the relation between a hypothetically heterogeneous  $D''$  and the internal structure of a plume conduit.

Finally, we had to restrict our modeling to a few examples of kilometer scale geochemical heterogeneities with simple shapes and basic spatial orientations, which are certainly poor representations of the great variety created by mantle stirring. As reviewed by Hofmann (2003) the spatial scale of heterogeneities may vary from  $10^2$ – $10^4$  km, to the decimeter scale (Allègre and Turcotte, 1986) and less. On the other hand, the kilometer-scale explored here is likely to be particularly relevant to mantle plumes, particularly in view of the rapid fluctuations in isotopic composition observed in the stratigraphic record of the Hawaiian Scientific Drilling Project (Eisele et al., 2003).

Our high resolution numerical model allows us to calculate deformations in a plume conduit with a detail that is not achieved in global mantle mixing models. Although such models have improved our understanding of convective stirring (see for example Kellogg, 1992; Davies, 2002; van Keken et al., 2003; Tackley, 2007, and references therein), it is important to focus on deformations inside hot, low viscosity and fast upwelling narrow plumes that are likely to represent unique places in the lower mantle where strain rates are particularly high and the associated stretching is more rapid and intense than elsewhere in the lower mantle.

This paper focuses on the basal thermal boundary layer feeding the plume and on the lower mantle part of the conduit, while, in a companion paper (in prep.) we model the dynamics of an upper mantle conduit sheared by a fast moving plate, allowing us to investigate how volcanoes sample a spatially heterogeneous plume conduit.

Lastly, we point out that although our results are used to elucidate the internal structure of the Hawaiian conduit, they may be of interest to other plumes, for example Galápagos, where isotope and incompatible element ratios have a complex spatial distribution, namely a horseshoe pattern with enriched signatures around a depleted center (White et al., 1993; Harpp and White, 2001). Interestingly, the observed asymmetrical spatial zonation of the Galápagos hotspot has persisted for several millions of years (Hoernle et al., 2000), suggesting the involvement of large scale heterogeneities in the source region feeding the plume.

## 2. Numerical model

We use the two dimensional code ConmanCYL (Farnetani, 1997; King et al., 1990) in cylindrical geometry to solve the equations of conservation of mass, conservation of momentum and conservation of energy for an incompressible viscous fluid at infinite Prandtl number. The size of the model domain is  $1500 \times 2890$  km in the radial and vertical directions, respectively. The element size is  $4 \times 4$  km in the regions of interest (i.e., the TBL and the plume conduit), elsewhere in the lower mantle the element size is  $8 \times 8$  km. At the top and bottom surfaces we impose free slip velocity boundary conditions and constant potential temperature  $T_{\text{top}} = 0$  °C,  $T_{\text{bot}} = 1800$  °C. The initial temperature condition is a constant potential temperature across the whole mantle  $T_m = 1300$  °C, except for the basal TBL where temperature increases as an error function profile. The potential temperature  $T$  is related to real temperature  $\theta$  through the relation:  $T = \theta \exp(-\alpha D / C_p)$ , where  $D$  is depth,  $C_p$  is the specific heat, and the other terms are given below. In the numerical model we use the following physical parameters: thermal expansion coefficient  $\alpha = 3.5 \cdot 10^{-5} \text{ K}^{-1}$ , mantle density  $\rho = 4000 \text{ kg m}^{-3}$  (for our buoyancy-driven flow we follow the Boussinesq approximation, therefore density variations due to temperature are considered only in the calculation

of the buoyancy force), thermal diffusivity  $\kappa = 10^{-6} \text{ m}^2 \text{ s}^{-1}$ , mantle depth  $D_m = 2900 \text{ km}$ ,  $g = 10 \text{ m s}^{-2}$ , lower mantle viscosity  $\eta_m = 10^{22} \text{ Pa s}$ , providing a Rayleigh number:

$$Ra = \frac{\rho g \alpha (T_{\text{bot}} - T_{\text{top}}) D_m^3}{\eta_m \kappa} = 6.1 \times 10^6. \quad (1)$$

The dependence of viscosity  $\eta$  on potential temperature  $T$  is:

$$\eta = \eta_m \exp \left[ \frac{E}{R} \left( \frac{T_m - T}{T_m T} \right) \right], \quad (2)$$

(Olson et al., 1993), where  $R$  is the gas constant and  $E = 300 \text{ kJ mol}^{-1}$  is the activation energy used for lower mantle diffusion creep (Karato and Wu, 1993). This exponential law gives  $\eta = 2 \times 10^{20} \text{ Pa s}$  for a plume excess temperature  $\Delta T_p = 200 \text{ }^\circ\text{C}$  and  $\eta = 10^{19} \text{ Pa s}$  for  $\Delta T_p = 400 \text{ }^\circ\text{C}$ , we note that three orders of magnitude viscosity reduction is also the minimum viscosity value we allow in the numerical model. Finally, to keep track of deformations induced by the plume flow we advect millions of passive tracers (i.e., not affecting the flow) both forward and backward in time. We use the velocity field calculated by the convection code and we advect the tracers with the robust and well tested two-dimensional bicubic spline interpolation by Akima (1996).

### 3. Results

Starting from the initial condition described above we run the calculation until the transient plume head reaches the base of the lithosphere and the velocity field approaches steady state. Fig. 1a (solid line) shows the vertical velocity component  $v_z$  as a function of radial distance  $r$  across the plume conduit at 2000 km depth: at the axis  $v_z^{\text{axis}} = 50 \text{ cm/yr}$ , at  $r = 38 \text{ km}$   $v_z = v_z^{\text{axis}}/2$  and at  $r = 70 \text{ km}$   $v_z = v_z^{\text{axis}}/10$ . The radial dependence of  $v_z$  is quite invariant throughout the height of the plume and it can be fitted by an exponential law  $v_z(r) = v_z^{\text{axis}} \exp(-Cr^2)$  where  $C$  is a constant. Such an exponential dependence on  $r^2$  is in excellent agreement with the analytical expression given by Olson et al. (1993). The significant radial variation of  $v_z$  generates high strain rates, in particular:

$$\dot{\epsilon}_{rz} = \frac{1}{2} \left( \frac{\partial v_z}{\partial r} + \frac{\partial v_r}{\partial z} \right) \quad (3)$$

which depends only on the first term, the second one being negligible in the conduit. We find that  $\dot{\epsilon}_{rz}$  tends to zero towards the plume axis, while it is maximum at  $r = 40 \text{ km}$  where  $\dot{\epsilon}_{rz}^{\text{max}} = 2 \times 10^{-13} \text{ s}^{-1}$  (Fig. 1a, long dashed line). We note that values of  $\dot{\epsilon}_{rz}$  of order  $10^{-13} \text{ s}^{-1}$  are extremely high, for comparisons strain rates in the asthenosphere are of order  $10^{-14} \text{ s}^{-1}$ . The plume buoyancy flux across the conduit surface  $S$  is:  $B = \rho \alpha (T - T_m) v_z S = 5.2 \times 10^3 \text{ kg s}^{-1}$ , a value in the range of present day hot-spot buoyancy flux, for example  $B_{\text{Hawaii}} = 8.7 \times 10^3 \text{ kg s}^{-1}$  and  $B_{\text{Iceland}} = 1.4 \times 10^3 \text{ kg s}^{-1}$  (Sleep, 1990). In Fig. 1a the dashed line showing the cumulative  $B$  as a function of  $r$  allows us to quantify that more than 50% of the buoyancy flux is carried in a zone where  $\dot{\epsilon}_{rz} > 10^{-13} \text{ s}^{-1}$  and that up to 75% is carried where  $\dot{\epsilon}_{rz} > 5 \times 10^{-14} \text{ s}^{-1}$ . In other words, most of the plume buoyancy flux occurs in highly sheared parts of the conduit. The most important effect of strain rates is to deform upwelling material. To quantify the deformations induced only by  $\dot{\epsilon}_{rz}$  in the conduit we consider an ideal radial alignment of 10 km diameter ‘circles’<sup>1</sup> initially at  $D = 2300 \text{ km}$ . At this depth the deformations are only due to  $\dot{\epsilon}_{rz}$ , while  $\dot{\epsilon}_{zz}$  is negligible, as we will show later (i.e. inset of Fig. 3 showing that  $\partial v_z / \partial z$  is

<sup>1</sup> We use the term ‘circles’ since we refer to a two-dimensional  $r$ - $z$  section and neglect the azimuthal direction  $\theta$ . The azimuthal size  $d\theta$  of the modelled heterogeneities could take any value from  $360^\circ$  (a torus) to only a few degrees. Since passive heterogeneities do not affect the flow, the exact value of  $d\theta$  is irrelevant.

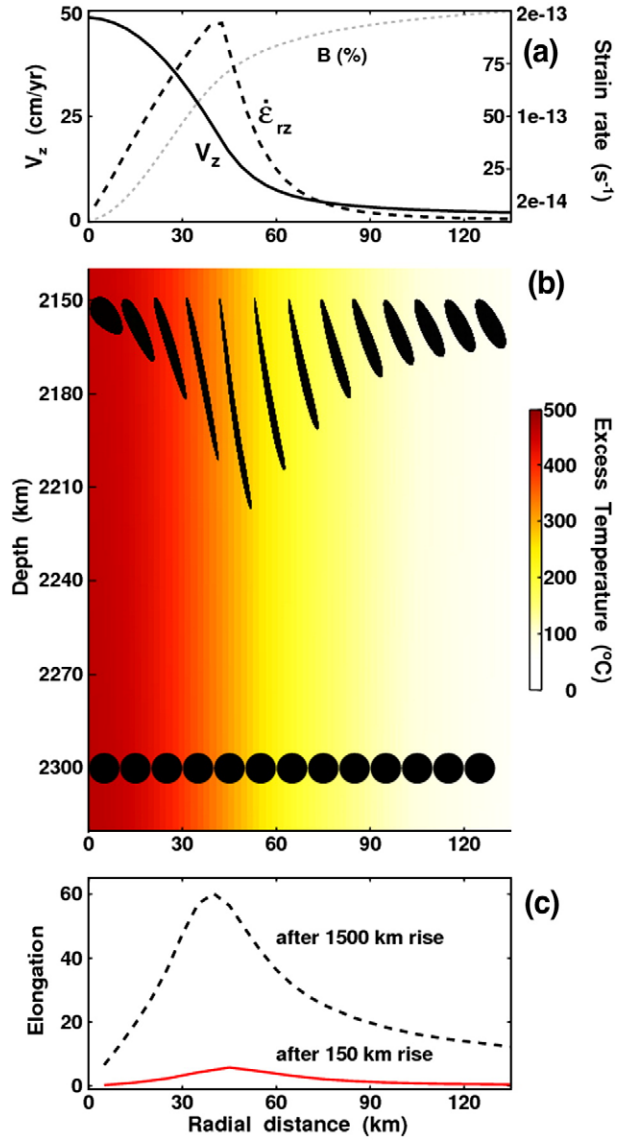


**Fig. 1.** (a) Radial profiles of vertical velocity  $v_z$  (solid line) and strain rate  $\dot{\epsilon}_{rz}$  (long dashed line) and cumulative buoyancy flux (short dashed line) note that 100% corresponds to  $B = 5.2 \times 10^3 \text{ kg s}^{-1}$ . (b) Sector of the plume conduit: initial ‘circular’ heterogeneities of 10 km diameter centered at  $D = 2300 \text{ km}$  and their shape after upwelling 150 km (at elapsed travel time: 0.31, 0.32, 0.37, 0.47, 0.72, 1.3, 2.1, 2.9, 3.7, 3.4, 4.9, 5.4, 6.0 Ma, respectively). (c) Radial profile of elongation for the heterogeneities shown above, after 150 km rise (red line) and after 1500 km rise (dashed line).

present only close to the stagnation point at the base of the plume). Fig. 1b shows the initial ‘circles’ and their shape after 150 km rise in the conduit: all of them have undergone vertical stretching and radial thinning, in particular the ones upwelling where  $\dot{\epsilon}_{rz}$  is high. To quantify the stretching we calculate the elongation:

$$e = \frac{l_f - l_i}{l_i}, \quad (4)$$

where  $l_i$  and  $l_f$  are the initial and final length, respectively. The elongation as a function of radial distance is shown in Fig. 1c, after 150 km rise in the conduit (red line), and after 1500 km rise (black line). For the latter case we find  $e^{\text{max}} = 60$  (i.e., for  $l_i = 10 \text{ km}$   $l_f = 70 \text{ km}$ ) and  $e^{\text{min}} = 5$  close to the axis. Clearly, ‘blob-like’ heterogeneities with initial aspect ratio 1:1 in a 2D-section cannot be preserved inside a plume conduit and only ‘filaments’ have a shape consistent with high strain rates.

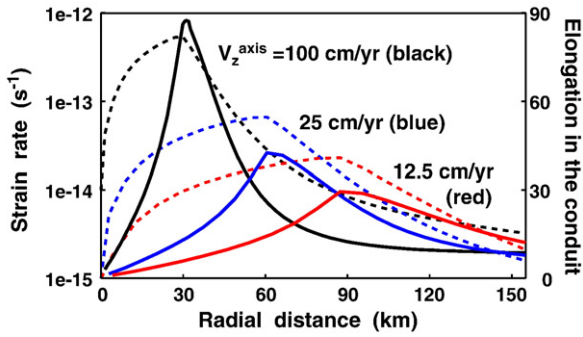


Fig. 2. Dashed lines: radial profile of strain rate  $\dot{\epsilon}_{rz}$  for a variety of vertical velocity profiles (see text). Solid lines: Radial profile of elongation, calculated after 1500 km rise in the conduit.

The results presented above depend on the vertical velocity field, which, in turn, depends on the assumed rheology and on the plume excess temperature (Farnetani, 1997), both of which are poorly constrained in the lower mantle. To investigate how the strain rate and the elongation vary as a function of the vertical velocity field we consider plume conduits that carry the same buoyancy flux as our reference model (with  $v_z^{\text{axis}} = 50$  cm/yr), but have higher or lower upwelling velocities. In the case of higher  $v_z$  (e.g.,  $v_z^{\text{axis}} = 100$  cm/yr) the conduit is narrower, thus the velocity gradients increase and  $\dot{\epsilon}_{rz}^{\text{max}} = 5.4 \times 10^{-13} \text{ s}^{-1}$  occurs at  $r = 30$  km only (Fig. 2, black dashed line) and  $e^{\text{max}} = 90$  (Fig. 2, black solid line). The elongation is non-negligible also close to the axis (e.g., at  $r = 10$  km  $e = 17$ ), ruling out the preservation of 1:1 aspect ratio heterogeneities even towards the plume center. A conduit with lower vertical velocities ( $v_z^{\text{axis}} = 25$  cm/yr and  $v_z^{\text{axis}} = 12.5$  cm/yr) will instead become broader than our reference model and the peaks of  $\dot{\epsilon}_{rz}$  and  $e$  shift towards the periphery (i.e.,  $60 < r < 90$  km). It is important to note that with low  $v_z$  the time required to travel a given distance is longer, so that, even if  $\dot{\epsilon}_{rz}$  is low, the elongation undergone while upwelling a given distance can be high ( $e^{\text{max}} = 30$ ) since  $e$  is directly proportional to  $\dot{\epsilon}_{rz}$  and to the time during which the strain rate operates.

We have no reason to rule out any of the velocity profiles considered above, for example thermo-chemical plumes may have broad conduits and  $v_z^{\text{axis}} = 10$  cm/yr (Farnetani and Samuel, 2005), while simulations of thermal plumes including strain weakening rheology (Larsen et al., 1999) and analytical models of chimney-like conduits 20 km diameter (Loper and Stacey, 1983) find axial upwelling velocity of 160 cm/yr and more. This range of uncertainty about possible upwelling velocities in mantle plumes should be kept in mind, however in the following we will use the velocity field of our reference model, hoping it may represent a plausible working hypothesis. Finally, we note that lower mantle velocities will increase by a factor of 3–4 in the upper mantle, due to the viscosity reduction (by a factor 10 to 100) between lower and upper mantle. In such case our reference model would give upper mantle upwelling velocities of order 150–200 cm/yr, which are in the range of those considered by Hauri et al. (1994) for olivine rheology.

### 3.1. Deformations in the thermal boundary layer and in the conduit

Studying the conduit dynamics is important but insufficient, since we cannot ignore the deformations undergone in the thermal boundary layer while plume material converges towards the conduit. Fig. 3a shows the evolving shapes of ‘circles’ 10 km diameter initially placed in the TBL at radial distance  $r = 400$  km and height  $H_i$  5.5, 25.5, 45.5, 65.5 km. The deformations result from the joint effect of three velocity gradients (maps of the velocity gradients are shown in the inset of Fig. 3): inside the TBL  $\partial v_r / \partial z$  reflects the decreasing radial velocity as a function of height above the free slip bottom boundary. In the zone

around the stagnation point, where  $v_z$  varies with height from the bottom value  $v_z = 0$  to the typical conduit values, the velocity gradient is  $\partial v_z / \partial z$ . Consequently, over a height of  $\sim 300$  km the strain rate  $\dot{\epsilon}_{zz}$  elongates material upwelling close to the axis. Finally, inside the conduit the dominant velocity gradient is  $\partial v_z / \partial r$ . By taking into account the whole deformation history we find horizontal shearing in the TBL due to  $\partial v_r / \partial z$ , further deformation occurs during the corner flow close to the axis due to  $\partial v_z / \partial z$  and intense vertical elongation occurs in the conduit due to  $\partial v_z / \partial r$ . Already at  $D = 2500$  km the 10 km diameter initial ‘circles’ are filaments 130–400 km long, allowing us to conclude that it is extremely unlikely to preserve 1:1 aspect ratios heterogeneities even in the lowermost part of the conduit.

The reader will notice that the 2D-surface of the heterogeneity is not constant, but it increases while approaching the plume axis. This is simply due to 3D-volume conservation in cylindrical geometry: a parcel of initial radial size  $dr_i$ , vertical size  $dz_i$  and azimuthal extent  $d\theta$  placed at radial distance  $r_i$  has an initial volume  $dV_i = dr_i dz_i r_i d\theta$ . After advection towards the plume axis  $d\theta$  is unchanged, while the final radial distance  $r_f < r_i$  therefore, the product of  $dr_f$  and  $dz_f$  has to increase.

Although the initial shape considered here is simplistic, it allows us to conclude that filaments are not confined to the peripheral part of the conduit, but are present also close to the axis. In other words, misleading conclusions can be drawn if we consider only the flow in the conduit and neglect the whole deformation history, including flow in the TBL.

### 3.2. Isolated lenses in the thermal boundary layer

We have considered initial ‘circles’ (in a  $r$ – $z$  section) which have the advantage of being simple and instructive, but are unlikely to be the prevalent shape of heterogeneities inside the TBL. We start by considering ‘lenses’ of elliptical shape of horizontal length  $AB = 100$  km and vertical height  $CD = 10$  km (i.e., aspect ratio 10:1), initially placed at  $r = 400$  km and with center at height  $H_i$  5.5, 25.5, 45.5, 65.5 km,

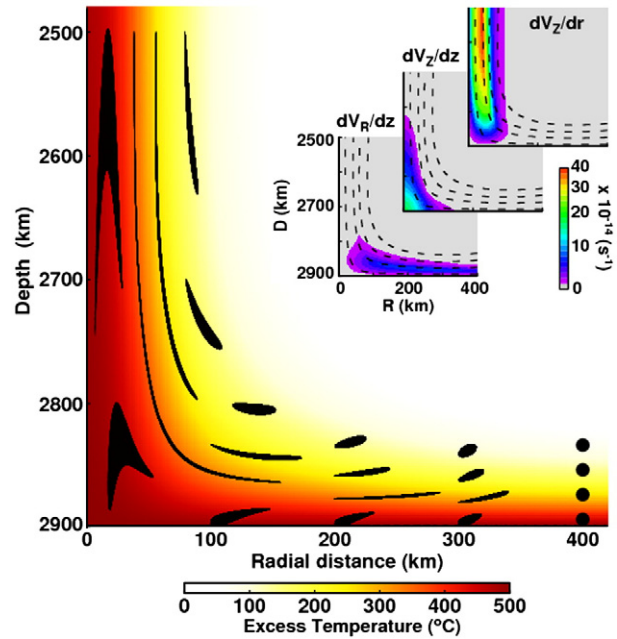
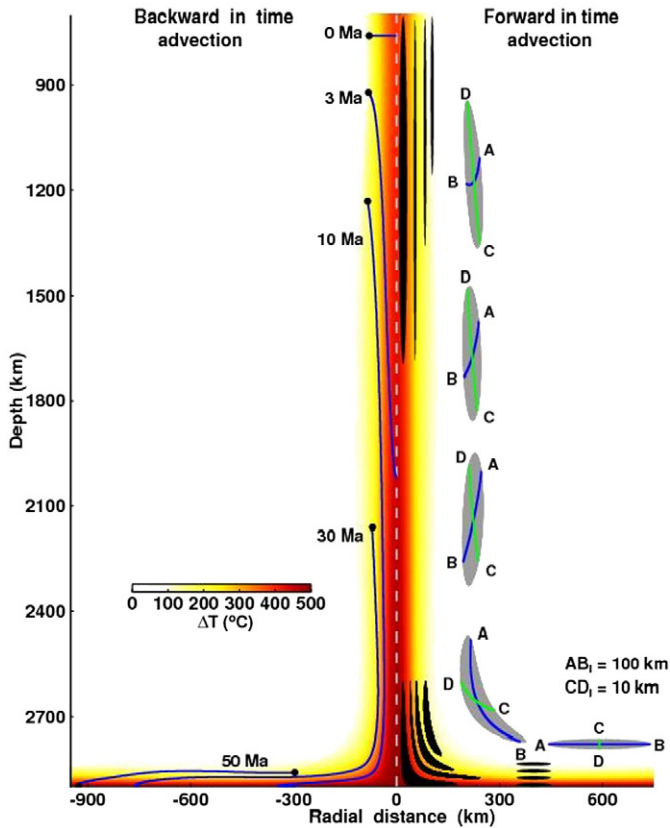


Fig. 3. Base of the conduit and TBL with initial ‘circular’ heterogeneities of 10 km diameter, centered at  $r = 400$  km and height  $H_i = 5.5, 25.5, 45.5, 65.5$  km. Heterogeneities are shown after elapsed travel time:  $t = 1.8, 3.6, 4.9, 6.0, 6.8$  Ma for  $H_i = 5.5$  km;  $t = 3.4, 5.7, 9.6$  Ma for  $H_i = 25.5$  km;  $t = 6.4, 11, 19$  Ma for  $H_i = 45.5$  km;  $t = 8.2, 15, 20.5, 24.7, 29.6$  Ma for  $H_i = 65.5$  km. Inset in the upper right shows maps of velocity gradients  $\partial v_r / \partial z$ ,  $\partial v_z / \partial z$  and  $\partial v_z / \partial r$ . Absolute values are used; note the non-progressive color scale. Dashed lines: fluid flow trajectories.



**Fig. 4.** Right side:  $100 \times 10$  km lenticular heterogeneities (black) shown: (i) in their initial position, at  $r = 400$  km and  $H_i = 5.5, 25.5, 45.5, 65.5$  km, (ii) entering the plume conduit at  $t = 5.5, 8.6, 17, 25$  Ma, (iii) reaching  $700$  km depth at  $t = 10.5, 22, 50.5, 79.5$  Ma. In grey: evolution of major (AB) and minor (CD) axis of lenses  $H_i = 65.5$  km during upwelling. For graphical reasons the radial axis is exaggerated. Left side: Backward advection of material initially at depth  $D = 760$  km. The front is shown after 3, 10, 30, 50 Ma.

(see right side of Fig. 4). The four ‘lenses’ are shown when they reach  $D = 2600$  km (the respective travel times are given in the figure caption) and when they reach  $D = 700$  km. For  $H_i = 5.5$  km the filament is centered at  $r = 15$  km, has a radial width  $w = 27$  km and length  $L = 980$  km. For  $H_i = 25.5$  km, the filament centered at radial distance<sup>2</sup>  $r = 50$  km has  $L = 1000$  km and  $w = 7.5$  km only, since its trajectory crosses zones with the highest velocity gradients. For  $H_i = 45.5$  km the filament is located at  $r = 76$  km, has a width  $w = 8$  km and  $L = 660$  km, while  $H_i = 65.5$  km becomes the most external filament at  $r = 96$  km with  $w = 9$  km and  $L = 430$  km. The final length and width depend on the deformations along the whole trajectory and on the requirement of 3D-volume conservation.

In Fig. 4 the grey ellipses are a radially exaggerated view of an upwelling lens ( $H_i = 65.5$  km), where we show the rotation of the axis AB and CD. During the corner flow the point D acquires the most internal position in the conduit, so that, relative to the other points, it rises at higher  $v_z$  and eventually reaches the tip of the filament. Instead point C always travels at a relatively low velocity (both  $v_r$  in the TBL and  $v_z$  in the conduit), so that it progressively lags behind and eventually reaches the bottom of the filament. The reason why the direction CD is the most stretched is because during the flow CD is roughly perpendicular to the main velocity gradients (i.e.,  $\partial v_r / \partial z$

<sup>2</sup> Radial distances are for the lower mantle, their extrapolation to the upper mantle requires to consider the ‘necking’ phenomenon induced by the viscosity reduction between  $\eta_{lm}$  and  $\eta_{um}$ . In the upper mantle  $v_z$  increases and to conserve flux, the conduit radius decreases. Using  $\eta_{um}/\eta_{lm} = (r_{um}/r_{lm})^4$ , for  $\eta_{um}/\eta_{lm} = 0.1$ ,  $r_{lm} = 30$  km corresponds to  $r_{um} = 16.9$  km, and  $r_{lm} = 60$  km to  $r_{um} = 33.7$  km.

in the TBL and  $\partial v_z / \partial r$  in the lowermost part of the conduit). The opposite happens for the direction AB which instead shrinks to a few kilometers.

The considerable length (450–1000 km) of the filaments has an important implication: filaments are ‘long lived’ structures and their geochemical fingerprint persists for a long time at a given radial distance. The transit time  $\tau$  represents the time it takes for the entire filament to transit across a given depth (e.g.,  $D = 700$  km).  $\tau$  is directly proportional to  $L_{\text{filament}}$  and inversely proportional to  $v_z$ , for the four filaments we find  $\tau = 3.4, 13.6, 15.7, 11.2$  Ma, respectively. These long time scales, even though they do not directly correspond to the transit time in the upper mantle zone of partial melting, allow us to speculate that the geochemical fingerprint of a given filament might be sampled by more than one volcano, as has been observed on the Island of Hawaii, where the same location above the plume is successively sampled by 0.5 Ma old Mauna Kea and recent Kilauea lavas bearing the same isotopic fingerprint (Abouchami et al., 2005).

### 3.3. Backward in time advection

Up to now our approach has been to select volumes of material initially in the TBL and to advect them forward in time. We now change perspective to the point of view of an observer registering the compositional structure of a plume at a given level in the conduit. We select material located *simultaneously* in the plume conduit at a given depth, and we advect it backward in time to explore its shape once traced back to the source region. Fig. 4 (left side) shows the backward advected front, initially located at  $760$  km depth (0 Ma), at elapsed times of 3, 10, 30, and 50 Ma. Already after 3 Ma the depth difference between the axial and the peripheral portions of the conduit is more than  $800$  km, implying that material ‘side by side’ in the conduit at a given time was at significantly different depths only a few million years before, in agreement with pipe flow models by Eisele et al. (2003). After 50 Ma the front is entirely traced back to the TBL, where its radial extent is  $>600$  km, and its flattened shape is governed by the velocity field: fast travelling material (low in the TBL) has to start further away from the plume axis to join slow travelling material (high in the TBL).

Fig. 5 shows the initial radial distance in the conduit vs. the ‘final’ radial distance once in the TBL. We note that the peripheral part of the conduit (e.g.,  $50 < r_{\text{in conduit}} < 80$  km) gathers material that was  $\sim 400$  km far apart, when traced back to the TBL. Although these numerical values depend on the calculated velocity field, which is probably simplistic, it appears that vigorous plumes are able to sample, and to bring side by side, very distant portions of their source region. It is also interesting to note that the tracer initially closest to the axis ( $r_{\text{in conduit}} = 1$  km) is advected back to  $r_{\text{in TBL}} = 900$  km. By contrast, an ideal axial tracer at  $r_{\text{in conduit}} = 0$  km would be traced back to the stagnation point  $(r, z) = (0, 0)$  at the base of the plume. What happens in the extreme vicinity of the axis will be investigated analytically in the supplementary online material.

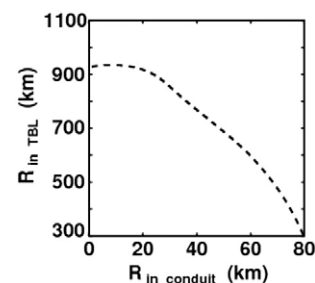


**Fig. 5.** Initial radial distance in the conduit, vs. radial distance once traced back in the TBL (e.g., after 50 Ma).

### 3.4. Spatial geochemical gradients and time fluctuations in the conduit

Although the distribution of heterogeneities inside the TBL is unknown we now consider some very simple TBL architectures, where the heterogeneities are not isolated, but form ‘trains’, of distinct lenses. This thought experiment allows us to study the dynamics of lenses with different spatial orientations: vertically elongated lenses (Fig. 6a) have horizontal axis  $AB_V=5$  km, and vertical axis  $CD_V=10$  km (0.5:1 aspect ratio), while for horizontally elongated lenses (Fig. 6b)  $AB_H=10$  km,  $CD_H=5$  km (1:0.5 aspect ratio). In the TBL equal volume heterogeneities are assumed to have a constant radial spacing of 30 km, and center at initial height  $H_i$  5.5, 25.5, 45.5, 65.5 km.

The conduit internal structure is composed of trains of filaments, and since  $CD_H=0.5 CD_V$ , it is not surprising that the filaments length  $L_H$  (e.g.,  $L_H=200, 400, 240, 120$  km, respectively, see right side of Fig. 6c) is roughly half of  $L_V$  (e.g.,  $L_V=330, 800, 470, 250$  km, respectively, see left side of Fig. 6c). It is interesting to note that only close to the axis the filaments remain isolated, elsewhere in the conduit the velocity gradients are such that the fastest point of lens  $\Psi$  travels faster than the slowest point of lens  $\Omega$ , so that the tip and the tail of several lenses may be simultaneously present in the conduit at a given depth. If we assume that the lenses have a distinct geochemical fingerprint this fine structure has two important implications: First, it generates high spatial geochemical gradients, mainly if we consider that the minimum filament radial width is  $w_H=1$  km and  $w_V=$

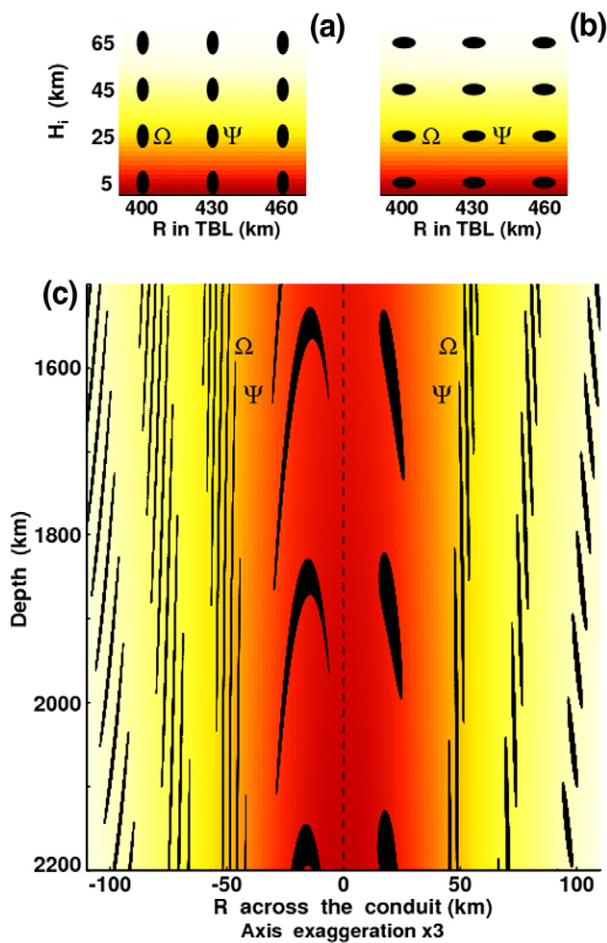


**Fig. 6.** (a) Ideal TBL structure with trains of equal volume, vertically elongated lenses  $5 \times 10$  km. (b) The same but for horizontally elongated lenses  $10 \times 5$  km. (c) Conduit structure (note radial axis exaggeration) for initial condition (a) at the left side, and for initial condition (b) at the right side.

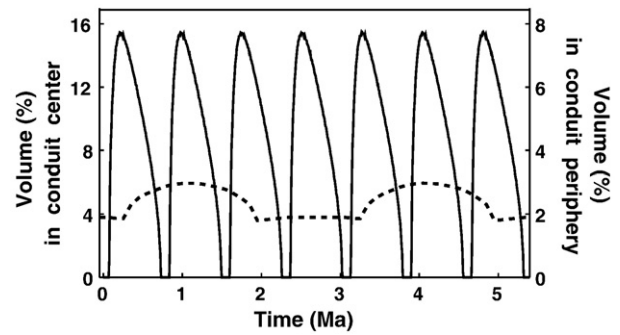


**Fig. 7.** Time fluctuations for the volume proportion of heterogeneous (filament) material upwelling in the conduit center,  $r < 30$  km (solid line), and in the periphery,  $90 < r < 120$  km (dashed line). Time fluctuations for initial lenses horizontally elongated (shown) are similar to those for initial lenses vertically elongated (not shown).

0.5 km. While it is not certain that partial melting and successive storage of melts in a large magma chamber would preserve the record of a few hundred meter scale heterogeneities, we speculate that this fine structure could be ‘sampled’ by magmatic melt inclusions and that it might explain the extreme geochemical heterogeneity often seen in such inclusions (Sobolev et al., 2000). Second, this conduit structure generates time fluctuations of an ideal ‘geochemical record’, as registered over time at a given radial distance. For example, if we examine the volume flux crossing a given level (say a depth of 1600 km) over a given range of capture radii, say from 0 to 30 km and 90 to 120 km, we find that the volume fraction of filament material fluctuates in a regular manner depending on the radial position within the plume. In particular, in the central part of the plume ( $r < 30$  km) the fluctuations have a period of less than 1 Ma and amplitude up to 15% for initially horizontally elongated lenses, as shown in Fig. 7 (solid line). The strong and rapid fluctuations correspond to the transit of distinct filaments, while the time periodicity depends on the initial spacing of the heterogeneities (i.e., if the initial spacing is doubled, then also the time interval between peaks doubles). In the peripheral part of the conduit (e.g.,  $90 < r < 120$  km) instead time fluctuations have a longer period and smaller (1–2%) amplitudes, as shown in Fig. 7 (dashed line). This is not surprising, since in the periphery the upwelling velocity is low and the filaments have a narrow radial width.

In conclusion, if we assume trains of equal size heterogeneities initially in the TBL, our model predicts that the associated geochemical time fluctuations will have a shorter period and a larger amplitude at the conduit center than at its periphery. While this conclusion is general, the specific values provided in the example depend on the assumed initial size and spacing of the heterogeneities. Interestingly, rapid (i.e., time-scales of ka, not Ma) fluctuations in Pb isotopic composition are observed in the stratigraphic record of the Hawaiian Scientific Drilling Project (Eisele et al., 2003) and they seem to be more rapid and more intense as the volcano approaches the plume center.

### 4. Comparison with previous models of conduit structure and conclusion

The first conceptual model of conduit structure was suggested nearly fifteen years ago and is known as the ‘concentric zoning’ (Hauri et al., 1994; DePaolo and Stolper, 1996) whereby the plume center samples the deepest part of the TBL, while the conduit periphery either samples the upper part of the TBL (Farnetani et al., 2002; Bryce et al., 2005) or, in case of entrainment, it samples also the surrounding mantle (Hauri et al., 1996). Our simulations confirm one basic idea of the concentric model: an horizontally stratified TBL (Fig. 8a) maps into a concentric conduit (Fig. 8b). We notice that if the TBL is radially homogeneous then, the conduit geochemical fingerprint will not vary

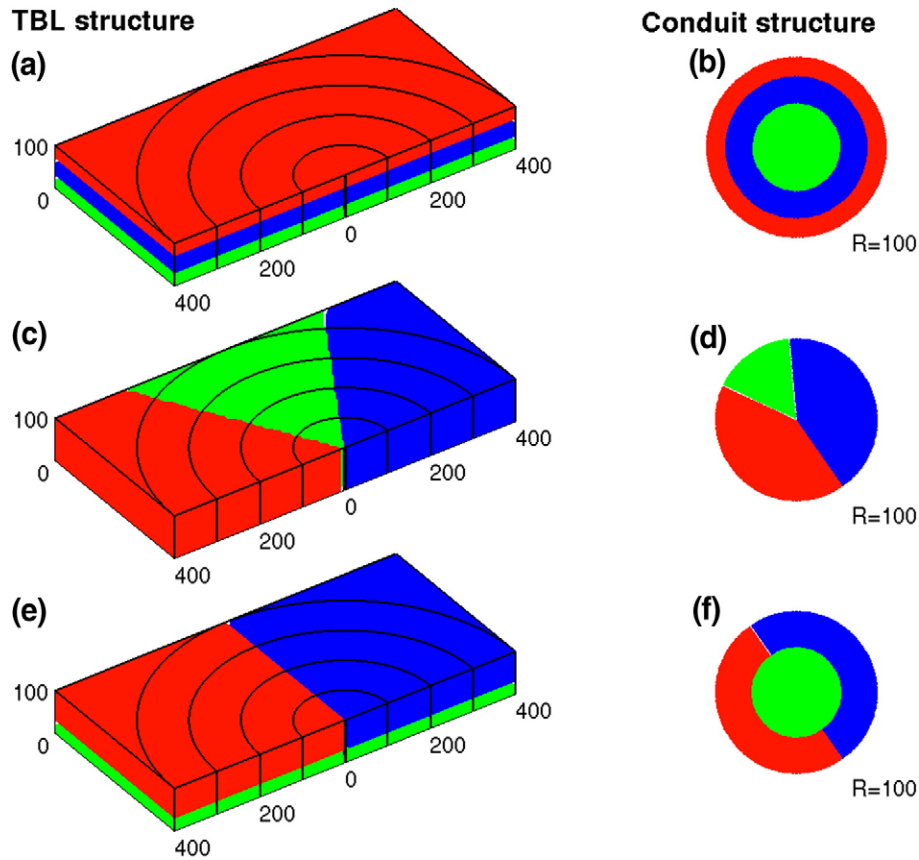


**Fig. 8.** (a,c,e) Schematic representation of TBL structure. (b,d,f) The corresponding conduit structure, which is time invariant. Colors are used to represent material with distinct isotopic fingerprint. 3D view of 2D-cylindrical axis-symmetric calculations.

over time. However, there are other schematic TBL architectures that would give rise to a time invariant structure: for example a purely azimuthally varying TBL (Fig. 8c) will map into a conduit with only azimuthal variability (Fig. 8d). This type of conduit structure is the one suggested by Kerr and Mériaux (2004), who concluded that the Hawaiian plume should be azimuthally, rather than concentrically zoned. We point out that the two above cases are not mutually exclusive but are end-members, so that all intermediate cases are possible, for example, in Fig. 8e a continuous deep layer is overlain by a bilaterally varying layer and the resulting conduit has both a radial and an azimuthal bilateral geochemical variability (Fig. 8f). This structure is likely to be responsible for the 'bilateral asymmetry' observed for consistent Pb isotopic differences between the Kea and Loa-trends of Hawaiian volcanoes (Abouchami et al., 2005) and for the roughly concentric distribution of  $^3\text{He}/^4\text{He}$  (DePaolo et al., 2001).

All models for a time invariant geochemical structure of the plume conduit implicitly assume that the geochemical variability in the TBL is restricted to the vertical and azimuthal directions, as shown in Fig. 8, while radial variations are excluded. Our paper goes beyond this simplifying assumption and explores the effect of finite-size heterogeneities in the TBL. We found that the resulting conduit structure varies spatially (i.e., both radially and azimuthally, according to the initial height and azimuthal extent of the finite-size heterogeneities) and temporally over time-scales ranging from a few to several millions of years, according to the initial size, shape and spatial orientation of the finite-size heterogeneities present in the TBL.

The conceptual model of conduit structure by Blichert-Toft et al. (2003) invokes a hypothetical 'plug-flow', whereby a broad core region with a nearly flat velocity profile is surrounded by a sheath with concentrated high-velocity gradients, strong shear flow and stretching. In the broad core region, there is little deformation so that any observed

heterogeneities resemble a stack of flat 'pancakes'. This model is not supported by our simulations, since the vertical velocity inside the plume conduit decreases exponentially with the square of radial distance, as in Olson et al. (1993). High strain rates are not confined to the conduit periphery, and most of the plume buoyancy flux occurs in highly sheared parts of the conduit. Moreover, we have shown that it is necessary to consider the entire deformation history of heterogeneities including their flow in the TBL towards the base of the plume. By doing so, it becomes clear that the existence of relatively undeformed heterogeneities is unlikely, even in the center of the plume and in the lowermost part of the conduit. By backward tracing a radial section of the conduit we demonstrated that plume material existing 'side by side' in the conduit at a given time, was at significant relative distance (several hundred kilometers) when traced back to the source region. For these reasons, we consider it highly unlikely to have 'horizontal pancakes' with the same geochemical fingerprint across the conduit. Our back-tracing results are also relevant for the interpretation of isotopic compositions of erupted lavas, which commonly show mixing relationships between isotopically different components that cannot be directly related by a common origin. Such a situation has been described by Eisele et al. (2003) for lavas from the HSDP drill core into Mauna Kea Volcano, where at least four isotopically distinct isotopic mixing end members were identified, which require distinct mantle histories.

Blichert-Toft et al. (2003) and especially Tanaka et al. (2008) have suggested time variations of the geochemical conduit structure. This is indeed possible and is consistent with the existence of finite-size heterogeneities in the TBL. For example, we have shown that lenses of initial size  $100 \times 10$  km once in the conduit, are stretched into 500–1000 km long filaments with a lower-mantle 'lifetime'  $\tau$  of order 3–11 Ma, while smaller scales lenses,  $10 \times 5$  km, have shorter  $\tau$  from less than a Ma to a few Ma. These different time-scales coexist and are

related, although in a complex way, to the size of heterogeneities in the TBL. Our results clearly indicate the importance of studying plume geochemical variability also over time scales of several millions of years. Tanaka et al. (2008) proposed that the entire Loa-type source in Hawaiian volcanoes is a temporal feature that may have appeared 3 Ma ago. Such time scales and the spatially important contribution of Loa-type geochemical fingerprint indeed suggest the presence of large scale heterogeneities in the source region. On the basis of our work in progress we can anticipate that a filament will preserve its elongated shape even once in the upper mantle, and that its transit in the sublithospheric melting zone will last a few million years. The first arrival of a distinct filament in the melting zone will induce a sudden change in the geochemical fingerprint of the active volcano sampling that specific portion of the plume head, subsequently, younger volcanoes sampling the same area will register the same geochemical fingerprint over a time period corresponding to the filament lifetime.

The results presented here show that deep seated heterogeneities are inevitably stretched into elongated filaments by processes starting in the TBL and accelerating in the plume conduit. Such ubiquitous filaments are consistent with the scenario proposed by Abouchami et al. (2005) to interpret the isotopic evolution of Mauna Kea lavas over the last 0.6 Ma. The formation of filaments also agrees with numerical simulations of thermal (Farnetani et al., 2002) and thermo-chemical (Farnetani and Samuel, 2005) plumes. The new contribution of the present work has been to quantify the relationship between the TBL architecture with finite-size heterogeneities and the spatio-temporal heterogeneous structure of the plume conduit. We have shown that isolated lenses of initial size  $100 \times 10$  km, once in the conduit, have lengths of order 500–1000 km and radial widths of 27–8 km. On the other hand, trains of small lenses of initial size  $10 \times 5$  km will form a fine structure in the conduit with high radial geochemical gradients and inducing time fluctuations with larger amplitude and higher frequency towards the conduit center with respect to the periphery. To our knowledge no previous fluid dynamically based work has shown the existence of such a fine heterogeneous structure in the plume conduit, yet this structure, ultimately derived from deep heterogeneities, could provide a framework to interpret short-term fluctuation of lava composition and high variability seen in magmatic melt inclusions.

Even though our purely thermal plume model represents almost certainly a gross oversimplification of a 'real' mantle plume, our model has revealed previously unsuspected features that offer significant promise in ultimately interpreting the complex geochemical record of lavas produced by such a plume. We will explore in subsequent contributions how the highly elongated heterogeneities generated by the plume flow may be sampled by a series of volcanoes carried across a melting plume by a moving lithosphere.

## Acknowledgements

We thank Bill White, Ross Kerr and an anonymous reviewer for their constructive and useful reviews. Erik Hauri provided thorough comments on an earlier version of the manuscript. CGF thanks Bernard Legras for discussions of the Supplementary Material and Claude Jaupart for support. We also wish to thank Rick Carlson for his editorial handling. IPGP Contribution No. 2489; LDEO Contribution No. 7247.

## Appendix A. Supplementary data

Supplementary data associated with this article can be found, in the online version, at doi:10.1016/j.epsl.2009.03.035.

## References

- Abouchami, W., Hofmann, A.W., Galer, S.J.G., Frey, F., Eisele, J., Feigenson, M., 2005. Pb isotopes reveal bilateral asymmetry and vertical continuity in the Hawaiian plume. *Nature* 434, 851–856.
- Akima, H., 1996. Algorithm 760: rectangular-grid-data surface fitting that has the accuracy of a bicubic polynomial. *ACM Trans. Math. Softw.* 22, 357–361.
- Allègre, C.J., Turcotte, D., 1986. Implications of a two component marble-cake mantle. *Nature* 32, 123–127.
- Blichert-Toft, J., Weis, D., Maerschalk, C., Agraniar, A., Albarède, F., 2003. Hawaiian hot spot dynamics as inferred from the Hf and Pb isotope evolution of Mauna Kea volcano. *Geochem. Geophys. Geosyst.* 4. doi:10.1029/2002GC000340.
- Boyet, M., Carlson, R.W., 2005.  $^{142}\text{Nd}$  evidence for early ( $>4.53$  Ga) global differentiation of the silicate Earth. *Science* 309, 576–581.
- Bryce, J.G., DePaolo, D.J., Lassiter, J.C., 2005. Geochemical structure of the Hawaiian plume: Sr, Nd, and Os isotopes in the 2.8 km HSDP-2 section of Mauna Kea volcano. *Geochem. Geophys. Geosyst.* 6. doi:10.1029/2004GC000809.
- Christensen, U.R., Hofmann, A.W., 1994. Segregation of subducted oceanic crust in the convecting mantle. *J. Geophys. Res.* 99, 19867–19884.
- Davaille, A., 1999. Simultaneous generation of hotspots and superswells by convection in a heterogeneous planetary mantle. *Nature* 402, 756–760.
- Davies, G.F., 2002. Stirring geochemistry in mantle convection models with stiff plates and slabs. *Geochim. Cosmochim. Acta* 66, 3125–3142.
- DePaolo, D.J., Stolper, E.M., 1996. Models of Hawaiian volcano growth and plume structure: implications of results from the Hawaii Scientific Drilling Project. *J. Geophys. Res.* 101, 11643–11654.
- DePaolo, D.J., Bryce, J.G., Dodson, A., Shuster, D.L., Kennedy, B.M., 2001. Isotopic evolution of Mauna Loa and the chemical structure of the Hawaiian plume. *Geochem. Geophys. Geosyst.* 2. doi:10.1029/2000GC000139.
- Eisele, J., Abouchami, W., Galer, S.J.G., Hofmann, A.W., 2003. The 320 ky Pb isotope evolution of the Mauna Kea lavas recorded in the HSDP-2 drill core. *Geochem. Geophys. Geosyst.* 4. doi:10.1029/2002GC000339.
- Farnetani, C.G., 1997. Excess temperature of mantle plumes: the role of chemical stratification across D". *Geophys. Res. Lett.* 24, 1583–1586.
- Farnetani, C.G., Legras, B., Tackley, P.J., 2002. Mixing and deformations in mantle plumes. *Earth Planet. Sci. Lett.* 196, 1–15.
- Farnetani, C.G., Samuel, H., 2005. Beyond the thermal plume paradigm. *Geophys. Res. Lett.* 32. doi:10.1029/2005GL022360.
- Garnero, E.J., McNamara, A.K., 2008. Structure and dynamics of Earth's lower mantle. *Science* 320, 626–628.
- Griffiths, R.W., Campbell, I.H., 1990. Stirring and structure in mantle starting plumes. *Earth Planet. Sci. Lett.* 99, 66–78.
- Harpp, K., White, W.M., 2001. Tracing a mantle plume: isotopic and trace element variations of the Galápagos seamounts. *Geochem. Geophys. Geosyst.* 2. doi:10.1029/2000GC000137.
- Hauri, E.H., Whitehead, J.A., Hart, S.R., 1994. Fluid dynamic and geochemical aspects of the entrainment in mantle plumes. *J. Geophys. Res.* 99, 24275–24300.
- Hauri, E.H., Lassiter, J.C., DePaolo, D.J., 1996. Osmium isotope systematics of drilled lavas from Mauna Loa, Hawaii. *J. Geophys. Res.* 101, 11793–11806.
- Hoernle, K., Werner, R., Phipps Morgan, J., Garbe-Schonberg, D., Bryce, J., Mrazek, J., 2000. Existence of complex spatial zonation in the Galápagos plume for at least 14 m.y. *Geology* 28, 435–438.
- Hofmann, A.W., 2003. Sampling mantle heterogeneity through oceanic basalts: isotopes and trace elements. In: Carlson, R. (Ed.), *Geochemistry of the mantle and core*, Treatise of Geochemistry, vol. 2. Elsevier, pp. 61–101.
- Hofmann, A.W., White, W.M., 1982. Mantle plumes from ancient oceanic crust. *Earth Planet. Sci. Lett.* 57, 421–436.
- Jellinek, A.M., Manga, M., 2004. Links between long-lived hotspots, mantle plumes, D" and plate tectonics. *Rev. Geophys.* 42. doi:10.1029/2003RG000144.
- Karato, S.I., Wu, P., 1993. Rheology of the upper mantle: a synthesis. *Science* 260, 771–778.
- Kellogg, L.H., 1992. Mixing in the mantle. *Annu. Rev. Earth Planet. Sci.* 20, 365–388.
- Kerr, R.C., Mériaux, C., 2004. Structure and dynamics of sheared mantle plumes. *Geochem. Geophys. Geosyst.* 5. doi:10.1029/2004GC000749.
- King, S.D., Raefsky, A., Hager, B.H., 1990. ConMan: vectorizing a finite element code for incompressible two-dimensional convection in the Earth's mantle. *Phys. Earth Planet. Inter.* 59, 195–207.
- Lassiter, J.C., DePaolo, D.J., Tatsumoto, M., 1996. Isotopic evolution of Mauna Koa volcano: results from the initial phase of the Hawaii Scientific Drilling Project. *J. Geophys. Res.* 101, 11769–11780.
- Larsen, T.B., Yuen, D.A., Storey, M., 1999. Ultrafast mantle plumes and implications for flood basalt volcanism in the Northern Atlantic Region. *Tectonophysics* 311, 31–43.
- Loper, D.E., Stacey, F.D., 1983. The dynamical and thermal structure of deep mantle plumes. *Phys. Earth Planet. Inter.* 33, 304–317.
- Murakami, M., Hirose, K., Kawamura, K., Sata, N., Ohishi, Y., 2004. Post-perovskite phase transition in  $\text{MgSiO}_3$ . *Science* 304, 855–858.
- Olson, P., Schubert, G., Anderson, C., 1993. Structure of axisymmetric mantle plumes. *J. Geophys. Res.* 98, 6829–6844.
- Samuel, H., Farnetani, C.G., 2003. Thermochemical convection and helium concentrations in mantle plumes. *Earth Planet. Sci. Lett.* 207, 39–56.
- Sleep, N.H., 1990. Hotspot and mantle plumes: some phenomenology. *J. Geophys. Res.* 95, 6715–6736.
- Sobolev, A.V., Hofmann, A.W., Nikogosian, I.K., 2000. Recycled oceanic crust observed in 'ghost plagioclase' within the source of Mauna Loa lavas. *Nature* 404, 986–990.
- Tackley, P.J., 2007. Mantle Geochemical Geodynamics. In: Bercovici, D., Schubert, G. (Eds.), *Mantle Dynamics, Treatise on Geophysics*, vol. 7. Elsevier, pp. 437–505.
- Tackley, P.J., 1998. Three-dimensional simulations of mantle convection with a thermo-chemical basal boundary layer: D"? In: Gunnis, M., Wyssession, M.E., Knittle, E., Buffett, B.A. (Eds.), *The Core–mantle Boundary Region*. AGU Geophys. Monogr. Ser., vol. 28, pp. 231–253.

- Tanaka, R., Makishima, A., Nakamura, E., 2008. Hawaiian double volcanic chain triggered by an episodic involvement of recycled material: constraints from temporal Sr–Nd–Hf–Pb isotopic trend of the Loa-type volcanoes. *Earth Planet. Sci. Lett.* 265, 450–465.
- Tolstikhin, I., Hofmann, A.W., 2005. Early crust on top of the Earth's core. *Phys. Earth Planet. Inter.* 148, 109–130.
- van Keken, P., Ballentine, C., Hauri, E.H., 2003. Convective mixing in the Earth's mantle. In: Carlson, R. (Ed.), *Geochemistry of the mantle and core. Treatise of Geochemistry*, vol. 2. Elsevier, pp. 471–491.
- White, W.M., McBirney, A.R., Duncan, R.A., 1993. Petrology and geochemistry of the Galápagos Islands: portrait of a pathological mantle plume. *J. Geophys. Res.* 98, 19533–19563.